Controlling Surface Morphology of Electrospun Polystyrene Fibers: Effect of Humidity and Molecular Weight in the Electrospinning Process

ARTICLE *in* MACROMOLECULES · DECEMBER 2003

Impact Factor: 5.8 · DOI: 10.1021/ma0351975

5 AUTHORS, INCLUDING:

John Rabolt
University of Delaware
249 PUBLICATIONS **9,699** CITATIONS

Controlling Surface Morphology of Electrospun Polystyrene Fibers: Effect of Humidity and Molecular Weight in the Electrospinning Process

Cheryl L. Casper,[†] Jean S. Stephens,[†] Nancy G. Tassi,[†] D. Bruce Chase,[‡] and John F. Rabolt*[,†]

Department of Material Science and Engineering and Delaware Biotechnology Institute, University of Delaware, Newark, Delaware 19716, and Dupont Central Research and Development, Experimental Station, Wilmington, Delaware 19880

Received August 13, 2003; Revised Manuscript Received September 30, 2003

ABSTRACT: Electrospinning is a technique used to produce micron to submicron diameter polymeric fibers. The surface of electrospun fibers is important when considering end-use applications. For example, the ability to introduce porous surface features of a known size is required if nanoparticles need to be deposited on the surface of the fiber or if drug molecules are to be incorporated for controlled release. Surface features, or pores, became evident when electrospinning in an atmosphere with more than 30% relative humidity. Increasing humidity causes an increase in the number, diameter, shape, and distribution of the pores. Increasing the molecular weight of the polystyrene (PS) results in larger, less uniform shaped pores. This work includes an investigation of how humidity and molecular weight affect the surface of electrospun PS fibers. The results of varying the humidity and molecular weight on the surface of electrospun PS fibers were studied using optical microscopy, field emission scanning electron microscopy (FESEM), and atomic force microscopy (AFM) coupled with image analysis.

Introduction

Electrospinning is a fiber spinning technique that produces materials with small fiber diameters, high surface area, and an interconnected fibrous network desirable for a range of applications. Current research efforts are focused on using electrospun fibers for filtration, chemical/biological resistant protective clothing, tissue engineering, and electronic applications.[1,2] A fundamental understanding of how to control the formation, shape, texture, and morphology of these fibers is essential. Determining the link between electrospinning parameters and electrospun fiber morphology will allow for the design of polymeric fibers to meet specific application needs.

The electrospinning technique, described extensively in the literature,[3−11] involves applying an electric field to a polymeric solution in order to produce micron to nanometer size fibers. The shape and surface morphology of the fibers depend on the electrospinning parameters used. The electrospinning process itself involves applying a high voltage to the tip of a syringe needle as shown in Figure 1. The increasing electric field causes the protruding droplet of polymer solution to deform due to electrostatic forces and causes the hemispherical droplet to become conical in shape, referred to as a Taylor cone. When the critical voltage is reached, the charge accumulated on the surface of the droplet due to the electric field overcomes the surface tension and an elongated fiber is forced downward to the grounded target. As the fiber travels toward the target, evaporation of the solvent occurs and the fiber is typically dry when arriving at the target.[12]

Humidity has been found to directly affect the surface morphology of electrospun fibers. Fibers electrospun from polystyrene (PS), polycarbonate (PC), and poly(methyl methacrylate) (PMMA) were found to contain submicron surface features when the polymers were dissolved in a volatile solvent and electrospun in the presence of humidity.[13] These surface features or "pores" resemble those seen in films.[14,15] Srinivasarao et al. observed the formation of a three-dimensionally ordered array of bubbles in a thin PS film. These structures were not observed when the films were formed in the absence of humidity. Since the pore formation was dependent upon a moist atmosphere and the use of a volatile solvent, the structures were considered to be breath figures.[14] Phase separation techniques have also been used to produce submicron structures as described by Van de Witte et al.[16]

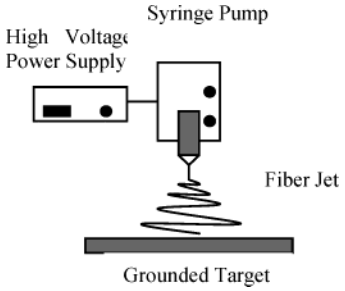

Figure 1. Schematic diagram of electrospinning setup.

The presence of pores on the surface of electrospun fibers can serve to increase the surface area for filtration applications, act as a cradle for enzymes, or be used to capture nanoparticles. Previous work completed in this lab has confirmed the existence of pores on the surface of electrospun fibers and the ability to fill these pores with silver nanoparticles.[13] The goal of this research is to study the effect of increasing humidity and varying molecular weight on pore size and distribution. Understanding the link between humidity and fiber morphology will allow for better control over the properties of electrospun fibers.

[†] University of Delaware.
[‡] Dupont.
* To whom correspondence should be addressed. E-mail: rabolt@udel.edu.

10.1021/ma0351975 CCC: $27.50
Published on Web 12/18/2003

Experimental Section

Polystyrene fibers were electrospun using a 35 wt % concentration of PS in tetrahydrofuran (THF) (HPLC; Fisher Scientific) for all of the experiments reported here. Molecular weights of the PS samples were 31 600, 171 000, 190 000, and 560 000 g/mol (Scientific Polymer Products). The polydispersity index (PDI) of the polymers was as follows: 1.09, 1.04, 3.00, and 1.04. A fifth PS sample (1.8×10^6 g/mol, 1.10 PDI) was investigated solely to assess whether the electrospinning process caused degradation of the molecular weight. All polymers dissolved at room temperature with 2 h of stirring.

The electrospinning apparatus consisted of a 5 mL syringe (Popper & Sons, Inc.) connected to a syringe pump (Orion Sage) that was encased in a vented Plexiglas box (2.5 ft × 2.5 ft × 3.5 ft). The syringe pump was used to supply a steady flow of 0.07 mL/min of solution to the tip of the needle. A high-voltage power supply (Glassman Series EH) was used to apply a potential of 10 kV to the syringe needle (Hamilton). The inner diameters of the needles used were 0.26 mm for the 31 600 g/mol solution, 0.51 mm for both the 171 000 and 190 000 g/mol solutions, and 1.60 mm for the 560 900 and 1.8×10^6 g/mol solutions. The target consisted of a grounded aluminum sheet placed 35 cm from the needle tip to ensure that the fibers were dry upon collection. The relative humidity (RH) was varied using a humidifier (Holmes HM-1700) placed inside of the electrospinning box. The temperature was kept at a constant 75−76 °F.

The electrospun PS fibers were characterized using optical microscopy (Olympus BX60) and FESEM (JEOL JSM-6330F and Hitachi S-4700). Fibers were directly spun onto SEM mounts then sputter-coated with gold for analysis. Pore size and distribution information was obtained from FESEM images using Scion Image Software. The micrographs used for these studies were acquired under the same magnification, electron beam density, and working distance.

AFM (Veeco Metrology Group Dimension 3100/ with Nanoscope IIIA control) investigations were performed under ambient conditions in tapping mode using TESP cantilevers. Electrospun fibers were analyzed on a double-sided carbon adhesive and scanned along the fiber length. Pore depth and surface area were calculated using manufacturer provided software. The 3 μm × 3 μm images were inverted, and particle size analysis was used to determine average pore depth. In order for the values to have statistical significance, more than 40 pores were measured per sample for pore depth analysis.

The molecular weight of the 1.8×10^6 g/mol PS was determined before and after the electrospinning process using gel permeation chromatography (GPC) (Water Alliance 2690). THF was used as the solvent for GPC analysis, and the detectors used were differential refractive index (Waters 410), viscometry (Viscotek), and multiangle light scattering (Wyatt Technology). All GPC data were acquired using Wyatt software and calculated directly from the scattering intensity of the eluting polymer.

Results

Varying Humidity Level. A 35 wt % solution of PS (190 000 g/mol, 3.0 PDI) dissolved in THF was electrospun under five different humidity ranges: <25%, 31−38%, 40−45%, 50−59%, and 60−72%. The humidity was the only factor varied during this experiment. At a humidity of less than 25%, the fibers were smooth and featureless as shown in Figure 2a. Increasing the humidity to 31−38% caused a visible difference in the surface morphology of the fiber. Figure 2b shows that the fiber surface contains a relatively small number of uniform, circular pores randomly distributed on the surface of the fiber. As the humidity increased from 31−38% to 40−45%, the shape of the pores remains the same, but they begin to heavily populate the fiber surface as shown in Figure 2c. The most dramatic difference is observed when the fibers are electrospun under 50−59% humidity. Figure 2d shows that at this increased humidity the pores are abundant on the surface of the fiber leaving little space between adjacent pores. The pores are no longer circular in shape due to the coalescence of smaller pores into larger, nonuniform shaped structures. Figure 2e shows that the pores obtained from the highest achievable humidity range, 60−72%, are also nonuniform in shape and are slightly larger than those obtained from the 50−59% humidity level.

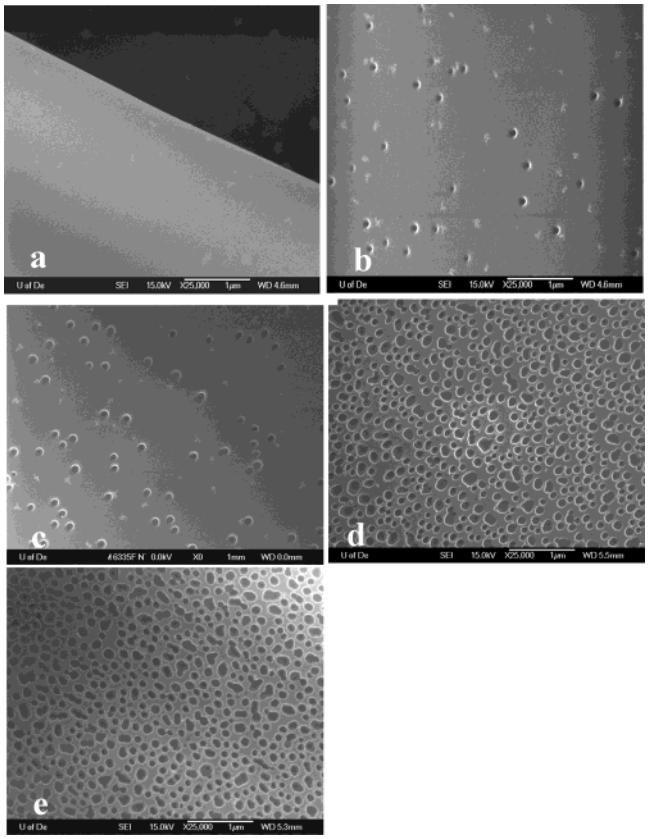

Figure 2. FESEM micrographs of 190 000 g/mol PS/THF fibers electrospun under varying humidity: (a) <25%, (b) 31−38%, (c) 40−45%, (d) 50−59%, (e) 60−72%.

Table 1. Pore Diameters of 190 000 g/mol PS/THF Fiber under Varying Humidity Levels

humidity range (%)	range of pore diameters (nm)	most frequent pore diameter (nm)
31−38	60−190	85
40−45	90−230	115
50−59	50−270	115
66−72	50−280	135

Figure 3a−d and Table 1 summarize the pore diameters and distributions observed at each humidity range as determined by image analysis. The data show that as the humidity increases, the pore diameter and pore size distribution both increase. The image software was also used to count the number of individual pores on the image. It was determined that for the humidity ranges of 31−38%, 40−45%, 50−59%, and 60−72% the numbers of pores observed on the images were 26, 56, 463, and 466, respectively, for a 4.5 μm × 3.75 μm area of each fiber. This confirms that the number of pores on the surface of the fiber increases with increasing humidity, which is evident in the FESEM images (Figure 2b−e). The 50−59% and 60−72% humidity levels had a similar number of pores on the surface. As the fiber surface becomes saturated with pores at the

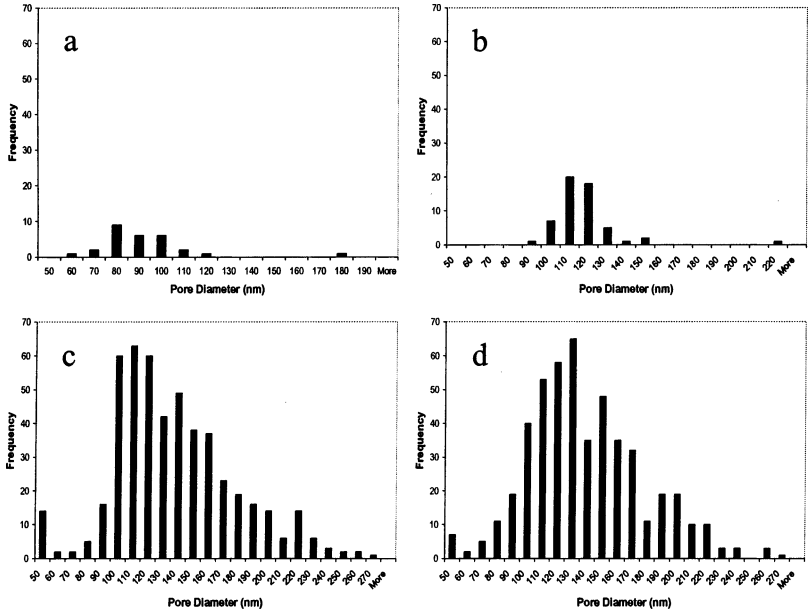

Figure 3. Pore diameter distributions of pores found on 190 000 g/mol PS/THF electrospun fibers at varying humidity ranges: (a) 31−38%, (b) 40−45%, (c) 50−59%, (d) 60−72%.

50−59% humidity range, further increases in humidity allow for only a small increase in the pore diameter and no significant increase in the number of pores.

Images obtained from the optical microscope and FESEM show that all of the fibers have a ribbonlike shape with a cross section of approximately 15 μm. It was shown that humidity does not affect the shape or diameter of the electrospun PS fiber in this experiment; these results do show that humidity has a large effect on the morphology of the fiber surface.

Previous studies of TEM cross sections of PS fibers suggested that the pores formed were surface specific and not networked through the fiber.[13] To confirm this observation and determine the effect of humidity on pore depth, AFM imaging was used to characterize the three-dimensional structure of the pores. Depth determinations were completed on the higher molecular weight, higher humidity samples. At lower humidity levels, the AFM tip radius was larger than the diameter of the pores preventing accurate probing of pore depths. Depths for the larger pores in these samples could be calculated but the numbers generated do not statistically represent the sample and thus will not be considered.

AFM measurements of the number of pores, their shape, and diameter are in agreement with the FESEM data. Additional information provided by AFM reveals that the depth of the pores increases as the humidity and molecular weight increase. For the 190 000 g/mol fibers, only the 60−72% humidity range could be analyzed for pore depths due to tip artifact issues previously mentioned. The average depth of these pores was determined to be 48 nm. The 560 900 g/mol fibers were determined to have an average pore depth of 171 nm at 50−59% humidity and 220 nm at the 60−72% humidity range. These values are within the standard deviation so it can be concluded that the pore depth did not significantly increase when going from 50−59% to 60−72% humidity. This again may be due to the fact that the fiber surface is already populated with pores at the 50−59% range so increasing the humidity further does not drastically change the pore diameter or pore depth. Upon comparison of the 60−72% humidity range for both the 190 000 and 560 900 g/mol fibers, it is evident that increased molecular weight greatly increases the depth of the pores from 48 to 220 nm.

AFM analysis allowed for the calculation of surface area of the porous PS fibers. The projected surface area for all the 3 μm × 3 μm images presented in Figure 4 is 9 μm^2. The calculated surface area for the images in Figure 4a−d is 12.4, 14.9, 10.67, and 12.1 μm^2, which is a 30−65% increase in the surface area of the fiber.

Varying Molecular Weight. Further investigations into humidity, molecular weight, and polydispersity effects on the surface features of electrospun fibers allowed for a more comprehensive look at the role of humidity in the electrospinning process. Polystyrene samples with molecular weights of 31 600 and 560 900 g/mol were used to study humidity and its effect on the electrospinning of high and low molecular weights of PS (PDI of 1.09 and 1.04, respectively). The previous PS sample (190 000 g/mol) contained a higher PDI of 3.0. Thus, to directly compare these samples, the differences in PDI had to be examined. To determine whether PDI played an integral role in pore formation or size, a similar molecular weight of 171 000 g/mol but a lower PDI of 1.04 was analyzed. The pore distribution charts and images are similar for the 171 000 and 190 000 g/mol solutions. As seen in Figure 5, the FESEM image of the pores produced from the 171 000 g/mol solution under 50−59% humidity is comparable to that for the 190 000 g/mol solution (Figure 2d). This shows that PDI does not greatly affect pore formation or pore size within the limits of this study. This also allows for a direct comparison of the fibers produced from 31 600, 190 000, and 560 900 g/mol solutions, regardless of the small differences in PDI values (1.09, 3.0, and 1.04, respectively).

Polystyrene with a molecular weight of 560 900 g/mol was used to study humidity and its effect on high molecular weight PS. The solution was electrospun under conditions similar to those described previously. However, because of the high viscosity of the solution, a needle with 1.60 mm inner diameter was used in order

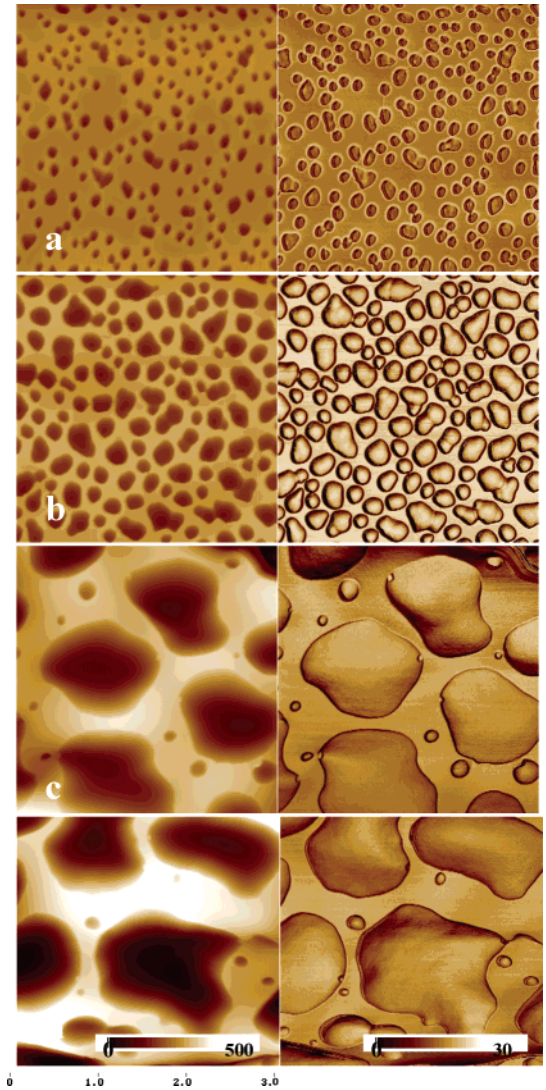

Figure 4. AFM images, topography (left), phase (right) (a) 190 000 g/mol PS fibers under 50−59% humidity, (b) 190 000 g/mol PS fibers under 60−72% humidity, (c) 560 900 g/mol PS fibers under 50−59% humidity, (d) 560 900 g/mol PS fibers under 60−72% humidity.

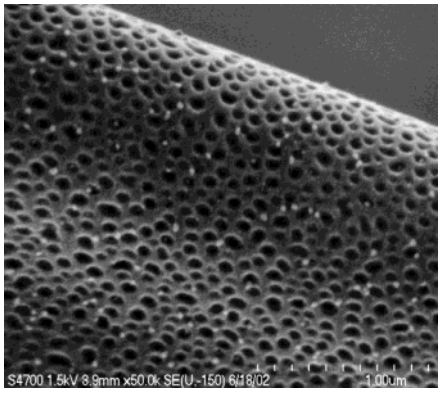

Figure 5. FESEM micrograph of 171 000 g/mol PS/THF fiber electrospun in 50% humidity.

to successfully electrospin this solution. Table 2 summarizes the average pore sizes obtained from these fibers. Figure 6a shows that a humidity range of 31−38% for the 560 900 g/mol solution produced a fiber with a significant number of circular pores with the most frequent pore diameter being 250 nm. This is significantly larger than the pores produced from the same

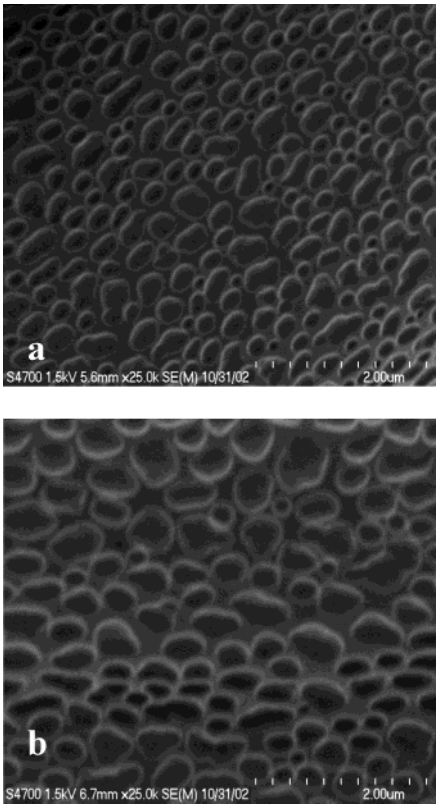

Figure 6. FESEM image of 560 900 g/mol fiber electrospun in (a) 31−38% humidity and (b) 40−45% humidity.

Table 2. Pore Diameters of 560 900 g/mol PS/THF Fiber under Varying Humidity Levels

humidity range (%)	range of pore diameters (nm)	most frequent pore diameter (nm)
31−38	150−650	250
40−45	150−600	350
50−59	100−850	300
60−72	200−1800	350

humidity using a 190 000 g/mol molecular weight solution. The higher molecular weight solution also resulted in a broader pore size distribution. The pore diameters varied in size from 150 to 650 nm for the 31−38% humidity range. Increasing the humidity to 40−45% resulted in an increase in pore diameter to 350 nm, as observed in Figure 6b. The pore size distribution remained relatively constant. Table 2 shows that increasing the humidity to 50−59% resulted in a broad pore size distribution but did not significantly affect the pore diameter (still approximately 300 nm). The largest pore size distribution was observed when the solution was electrospun under 60−72% humidity. Table 2 shows that pores from 200 to 1800 nm were found on the surface of the fiber electrospun under 60−72% humidity.

Comparing all humidity levels for the fibers produced from the 560 900 g/mol PS to that of the 190 000 g/mol PS shows that as the molecular weight of the polymer increases, both the diameter of the pores and the distribution of the pore sizes increase. Humidity has the same effect, independent of the polymer molecular weight, in that increasing the humidity causes an increase in the pore size and number of pores found on the surface. The higher molecular weight solution did not show a drastic increase in the number of pores on the surface as was observed in the 190 000 g/mol fibers since the pores are already large, and they begin to coalesce at higher humidity ranges.

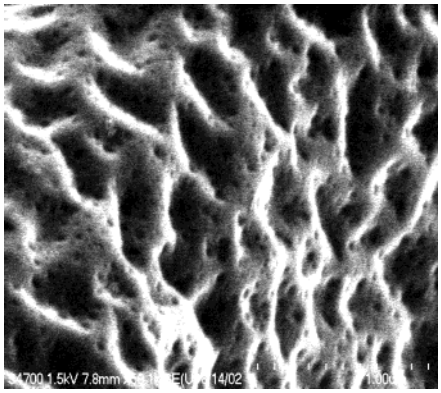

Figure 7. FESEM image showing micro- and nanopores on 31 600 g/mol PS/THF bead, 60−72% humidity.

Table 3. Micro- and Nanopore Diameters of 31 600 g/mol PS/THF Beads under Varying Humidity Levels

humidity range (%)	most frequent micropore diameter (nm)	most frequent nanopore diameter (nm)
40	179	26
52	292	58
56−62	343	92
66−72	384	71

Differences in the shape of the pores were found when comparing all of the 190 000 g/mol fibers to 560 900 g/mol (Figure 2b vs 6a). The 190 000 g/mol solution produced electrospun fibers that contained very uniform, circular pores. The 560 900 g/mol solution yielded fibers with irregularly shaped pores that appear elongated along the length of the fiber.

As discussed previously, both moderate (190 000 g/mol) and high (560 900 g/mol) molecular weights of PS were studied. For a complete comparison of molecular weight and humidity, a 35 wt % PS with a lower molecular weight of 31 600 g/mol was analyzed. This solution was electrospun under the same conditions indicated earlier with the exception that a smaller needle (0.26 mm inner diameter) was used. The lower molecular weight of the PS caused the solution to electrospray beads only, with no fibers being produced. The solution was electrospun under 40%, 52%, 56−62%, and 60−72% humidity ranges. The beads were approximately 20 μm in diameter independent of the humidity level. Pores were evident on the surface of the beads but looked different than those observed on the surface of the PS fibers in this study. The PS beads contained two regimes of pore sizes as shown in Figure 7. The term "micropore" will be used to indicate a porous structure with a diameter greater than 100 nm and "nanopore" to indicate a pore diameter of less than 100 nm. Increasing the humidity level produced the same effect as seen in the PS fibers; pores were more abundant and slightly larger in diameter at higher humidity levels. Table 3 summarizes the pore diameters on the surface of the PS beads. Electrospinning the 31 600 g/mol molecular weight PS in the presence of 40% humidity produced beads with a micropore size of 179 nm and a nanopore size of 26 nm. At 52% humidity, the micropore size increased to 292 nm and the nanopore diameter was 58 nm. The 56−62% humidity range produced micropores on the order of 343 nm and nanopores of 92 nm in diameter. The pore sizes increased again when the PS was electrospun under 60−72% humidity. The micropore size was found to be 384 nm and the nanopore diameter was 71 nm.

During the investigation of molecular weight and humidity, the question arose as to whether the electrospinning process degrades the molecular weight of the polymer. To address this issue, a very high molecular weight, 1.8×10^6 g/mol, PS was studied. GPC was performed on the PS before and after electrospinning. Before electrospinning, the number-average molecular weight of the bulk sample was determined to be 1.540×10^6 g/mol. A 12.2 wt % sample of PS/THF was made and electrospun under standard electrospinning conditions previously mentioned. The resulting fibers were then dissolved in THF and submitted for GPC analysis. After electrospinning, the molecular weight of the PS was 1.587×10^6 g/mol. This initial GPC analysis reveals that the electrospinning process does not degrade the molecular weight of PS. Hence, although high-stress conditions may be present during the electrospinning process and molecular orientation may result, the magnitude of the elongational flow is not enough to cause chain scission.

Discussion

The exact mechanism of pore formation is complex. Breath figures have been used to explain the formation of pores on electrospun fibers.[13] Breath figures form due to evaporative cooling that occurs as a result of solvent evaporating as the electrospinning jet is being propelled toward the target. The surface of the jet cools and water from the air condenses on the surface of the fiber. As the fiber dries, the water droplets leave an imprint behind.[13] Srinivasarao et al. use breath figures as an explanation for the presence of three-dimensional structures on a thin PS film.[14] In their work, a thin film was made by evaporating a PS solution in a volatile solvent and passing humid air across the surface of the film. The resulting film contained hexagonally ordered arrays of pores. The pores obtained on the surface of an electrospun fiber are not ordered arrays of uniformly shaped pores. The difference in breath figure pores and the pores on an electrospun fiber are most likely due to the motion and elongation of the jet through the moist air. Also, the fibers carry a charge that may affect the ordering of the pores and their density.[13] Thus, the formation of pores by the electrospinning process is a much more complex process with many variables to be considered.

The concept of breath figures alone does not fully explain the pore size differences seen when changing the molecular weight of the polymer. If pore formation was based solely on breath figures, pore size would primarily be a function of humidity and molecular weight would not play a major role in determining the size or shape of porous structures. Another possible mechanism for pore formation is phase separation. There are four main phase separation mechanisms to produce porous membranes: thermally induced phase separation (TIPS), immersion precipitation, air-casting of the polymer solution, and precipitation from the vapor phase.[17] A detailed discussion of each type of phase separation in relation to pore formation was previously published.[13] Thermodynamic instability is the driving force behind phase separation. Decreasing temperature, loss of solvent, or increase in nonsolvent causes a solution to become thermodynamically unstable.[18] During the electrospinning process, all three of these situations are encountered, thus making phase separation a likely contributing mechanism of pore formation.

Bognitzki et al. report the formation of pores due to phase separation in electrospun poly-L-lactide, polycarbonate, and polyvinylcarbazole when dissolved in dicholoromethane.[19] Thermally induced and vapor induced phase separations are the most pertinent phase separation processes to explain the pore formation in the PS/THF electrospun fiber. Vapor induced phase separation involves the penetration of a nonsolvent vapor causing phase separation of the polymer solution. In this case water is the nonsolvent, which induces the phase separation of the homogeneous mixture of PS and THF.[20] Rapid evaporation of the solvent as the jet is being projected from the needle causes lowering of the temperature on the fiber, thus making TIPS a viable explanation for pore formation as well. During the evaporation of solvent, pore formation begins when the temperature reaches the bimodal temperature and continues to grow until the crystallization temperature is reached.[21] Phase separation occurs by the mechanisms of nucleation and growth (NG) and/or spinodal decomposition (SD). Generally, an interconnected pore structure is characteristic of the NG mechanism while closed pores are produced by SD.[16,20] On the basis of structural features only, SD is the most probable mechanism for phase separation in the electrospinning of PS/THF fibers since early work in our lab indicated that there is no interconnectivity of the pores throughout the fiber interior.[13]

The molecular weight effects on pore formation could be due to phase separation or may be an issue of viscosity. Even though a 35 wt % solution was made of all three molecular weights, the 31 600 g/mol solution has a much lower viscosity than that of the 560 900 g/mol solution. Thus, differences in viscosity made it difficult to determine whether changes in pore size and shape are due to molecular weight effects or differences in viscosity of the solutions. Research is currently in progress to investigate this issue.

It is evident that neither the phase separation theory nor the formation of breath figures alone fully explains the phenomena of pore formation in electrospun PS fibers. Rather, the porous surface of electrospun fibers is due to combination of both phase separation and breath figure formation.

Conclusions

It has been demonstrated that the amount of moisture in the air affects the surface morphology of electrospun PS fibers from THF. Electrospinning in an atmosphere of less than 25% humidity produced smooth fibers without any surface features. When the humidity is above 30%, pores begin to form on the surface of the fiber. Increasing the amount of humidity causes an increase in the number of pores on the surface, the pore diameter, and the pore size distribution. Higher molecular weight solutions cause fibers to contain larger pores that are less uniform in shape and size. Minor differences in PDI did not affect pore size or distribution. The presence of humidity did not influence the fiber shape or diameter. GPC measurements of an ultrahigh molecular weight PS (1.8×10^6 g/mol) before and after electrospinning indicated that the electrospinning process does not degrade the polymer chains of PS.

These insights provided by this work gave us a stronger fundamental understanding of the electrospinning process. The ability to produce electrospun fibers with tailorable surface features will allow fibers to be customized for specific uses such as filtration, tissue engineering, and drug delivery.

Acknowledgment. The authors thank NSF (NIRT and DMR) and DOE PAIR for financial support of this work. We also thank Dr. Kirk Czymmek, Debbie Powell, and Gerald Poirier for their expertise in FESEM and TEM. Dr. Silke Megelski for her insight in electrospinning. Colin Baker for his assistance with image analysis software and Kip Chase for help with the electrospinning setup. A special thank you to Dr. Patricia Cotts (Dupont CR&D) for GPC analyses.

References and Notes

(1) Deitzel, J. M.; Kleinmeyer, J.; Harris, D.; Tan, N. C. B. *Polymer* **2001**, *42*, 261−272.
(2) Gibson, P.; Schreuder-Gibson, H.; Rivin, D. *Colloids Surf., A* **2001**, *187*, 469−481.
(3) Doshi, J.; Reneker, D. H. *J. Electrost.* **1995**, *35*, 151−160.
(4) Fong, H.; Chun, I.; Reneker, D. H. *Polymer* **1999**, *40*, 4585−4592.
(5) Bognitzki, M.; Frese, T.; Wendorff, J. H.; Greiner, A. *Abstr. Pap. Am. Chem. Soc.* **2000**, *219*, 173-PMSE.
(6) Koombhongse, S.; Liu, W. X.; Reneker, D. H. *J. Polym. Sci., Part B: Polym. Phys.* **2001**, *39*, 2598−2606.
(7) Reneker, D. H.; Chun, I. *Nanotechnology* **1996**, *7*, 216−223.
(8) Srinivasan, G.; Reneker, D. H. *Polym. Int.* **1995**, *36*, 195−201.
(9) Schreuder-Gibson, H.; Gibson, P.; Senecal, K.; Sennett, M.; Walker, J.; Yeomans, W.; Ziegler, D.; Tsai, P. P. *J. Adv. Mater.* **2002**, *34*, 44−55.
(10) Matthews, J. A.; Wnek, G. E.; Simpson, D. G.; Bowlin, G. L. *Biomacromolecules* **2002**, *3*, 232−238.
(11) Jaeger, R.; Bergshoef, M. M.; Batlle, C. M. I.; Schonherr, H.; Vancso, G. J. *Macromol. Symp.* **1998**, *127*, 141−150.
(12) Fong, H.; Liu, W. D.; Wang, C. S.; Vaia, R. A. *Polymer* **2002**, *43*, 775−780.
(13) Megelski, S.; Stephens, J. S.; Chase, D. B.; Rabolt, J. F. *Macromolecules* **2002**, *35*, 8456−8466.
(14) Srinivasarao, M.; Collings, D.; Philips, A.; Patel, S. *Science* **2001**, *292*, 79−83.
(15) Limaye, A. V.; Narhe, R. D.; Dhote, A. M.; Ogale, S. B. *Phys. Rev. Lett.* **1996**, *76*, 3762−3765.
(16) VandeWitte, P.; Dijkstra, P. J.; vandenBerg, J. W. A.; Feijen, J. *J. Membr. Sci.* **1996**, *117*, 1−31.
(17) Matsuyama, H.; Teramoto, M.; Nakatani, R.; Maki, T. *J. Appl. Polym. Sci.* **1999**, *74*, 171−178.
(18) Wijmans, C. A. S. J. G. In *Preparation of Asymmetric Membranes by the Phase Inversion Process*; Bungay, P. M., e. a., Ed.; D. Reidel Publishing Co.: Dordrecht, The Netherlands, 1986; p 39.
(19) Bognitzki, M.; Czado, W.; Frese, T.; Schaper, A.; Hellwig, M.; Steinhart, M.; Greiner, A.; Wendorff, J. H. *Adv. Mater.* **2001**, *13*, 70.
(20) Park, H. C.; Kim, Y. P.; Kim, H. Y.; Kang, Y. S. *J. Membr. Sci.* **1999**, *156*, 169−178.
(21) Matsuyama, H.; Maki, T.; Teramoto, M.; Asano, K. *J. Membr. Sci.* **2002**, *204*, 323−328.

MA0351975